The 14th World Conference on Earthquake Engineering
October 12-17, 2008, Beijing, China

An estimation method of frequency response functions and its application to microtremor

Masataka NAKAMURA[1], Jun-ichi SUZUMURA[2] and Kazufumi HANADA[3]

[1] *Research associate, Dept. of Civil Eng., Coll. of Sci. and Tech., Nihon University, Tokyo, Japan*
[2] *Assistant professor, Dept. of Civil Eng., Coll. of Sci. and Tech., Nihon University, Tokyo, Japan*
[3] *Professor, Dept. of Civil Eng., Coll. of Sci. and Tech., Nihon University, Tokyo, Japan*
Email: masa@civil.cst.nihon-u.ac.jp

ABSTRACT :

In microtremor observation, forces are inputted to multipoint of the system. However, input forces cannot be specified. The authors have proposed a new method to estimate Frequency Response Functions, which is a scheme to extract coherent components of the system non-parametrically. This paper presents the availability of the proposed method for applying to microtremor records of an existing bridge. Consider items are as follows. (1)The modal characteristics identified by the proposed method in combination with an experimental modal analysis method, (2)comparison with results of forced vibration tests (FVTs), and (3)comparision with results of eigenvalue analysis of numerical model referred to FVT results.

KEYWORDS: frequency response functions, multipoint observation system, modal characteristics, an existing bridge, microtremor observation records, output only data

1. INTRODUCTION

It is necessary to estimate dynamic behaviors of a subject structure system with high precision and to obtain the dynamic characteristics of the physical model for earthquake resistant design. In microtremor observation, dynamic behaviors of the subject system can be observed during its in-service. It can also be expected to separate close modes by an appropriate data processing scheme, since forces are inputted to multipoint of the system. Furthermore, the observation activity is able to be carried out without artificial vibration sources. However, input forces for the system are unknown and cannot be specified, and the Signal/Noise (S/N) ratios of the observed records are generally small. In the current scheme, such as Operational Modal Analysis (OMA), unknown inputs are assumed to be white. The scheme is not self-contained but to be followed by Frequency Domain Decomposition (Brincker R., et al. 2000) or Stochastic Subspace Identification (Peeters B., et al. 1999). In the case that Free-Decay is parametrically estimated (B. Schwarz, et al. 2007 and Farrar, C.R., et al. 1997), modal characteristics are identified with experimental modal analysis (EMA) methods which have been often applied.
On the other hand, an estimation method of the Single-Input Single-Output (SISO) system transfer function (H_1 estimation, H_2 estimation, H_v estimation) has been also applied often (M. Izumi, et al. 1990), for which a relation between input and output of two observation points is treated as a spectral ratio between them from multiple observation recording in the system. H_1, H_2 and H_v estimation are estimated as observed values with noise contamination in the output, the input and the input/output, respectively. H_v estimation is represented by a geometric average of H_1 estimation and H_2 estimation (G.T. Rocklin., et al. 1985). The obtained transfer function varies significantly depending on the evaluation of noise in observed values. The vibration amplitude of the transfer function estimated with these methods satisfies a relation of $|H_1| \le |H_2| \le |H_v|$. Input and output of the SISO system are considered to be the output signals of a Single-Input Multiple-Output (SIMO) system under some input, which may be colored. The transfer function of the SISO represents the Frequency Response Function (FRF) of the SIMO.
The authors have proposed a new method to estimate FRFs, which is a scheme to extract coherent components of a subject system non-parametrically from the system's response records with unknown input force and small the S/N ratios. In the proposed method, the authors mention as follows, (1)the total amount of noise from all measurement points is estimated as a base for measured values with a large amount of noise such as earthquake and microtremor records, (2)whitening property is not assumed in the input, and (3)applications to a multipoint response measurement are considered.

These three points are set as a base for the processing. This paper presents the availability of the proposed method for applying to microtremor records of an existing bridge. Considered items are as follows. (1)The modal characteristics identified by the proposed method in combination with an EMA method, (2)comparison with results of Forced Vibration Tests (FVTs), and (3)comparision with results of eigenvalue analysis of numerical model referred to FVT results.

2. THE THEORY OF THE PROPOSED METHOD

In this paper, ω in the following equations is omitted because all functions are variable as frequency domain. It is assumed that the noise included data at a measuring point is independent of other measurements.

2.1.Definition of FRF

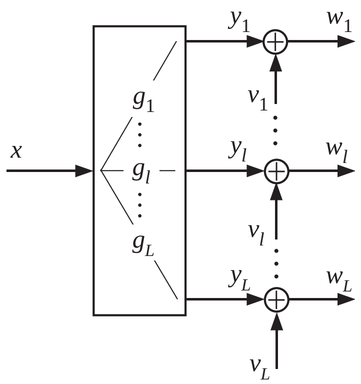

Figure 1 The Single-Input Multiple-Output system.

A SIMO system is shown in Figure 1. A linear relationship holds between the input signal x and the output signal y_l at point l as follows,

$$y_l = g_l x \quad (l = 1 \sim L), \tag{2.1}$$

where g_l represents the complex-valued transfer function. As output signal at point 1 is reference, ratio of output signals can be written as,

$$y_l / y_1 = g_l / g_1 = h_l \, . \tag{2.2}$$

Eqn.2.2 represents the ratio of output signals in the SIMO system. In this paper, we define h_l in Eqn.2.2 as the FRF of the objective point l with respect to the reference point 1.

2.2.The Theory of the Proposed Method for Estimating FRF (M.Nakamura, et al. 2006)

Generally, microtremor record includes noise. As N times measurements are carried out, the measuring data $\mathbf{w}_l$ at point l and an input signal $\mathbf{x}$ can be written as,

$$\mathbf{w}_l = \mathbf{y}_l + \mathbf{v}_l \in C(N \times 1), \tag{2.3}$$

$$\mathbf{y}_l = \left\{ y_l^{(1)} \ \cdots \ y_l^{(N)} \right\}^T, \ \mathbf{v}_l = \left\{ v_l^{(1)} \ \cdots \ v_l^{(N)} \right\}^T, \ \mathbf{w}_l = \left\{ w_l^{(1)} \ \cdots \ w_l^{(N)} \right\}^T, \ \mathbf{x} = \left\{ x^{(1)} \ \cdots \ x^{(N)} \right\}^T, \tag{2.4}$$

where the number in parentheses of Eqn.2.4 denotes the measuring times number $(n = 1 \sim N)$, and T denotes the transposition. The measuring data at points j and k can be written as,

$$\mathbf{w}_j = g_j \mathbf{x} + \mathbf{v}_j, \quad \mathbf{w}_k = g_k \mathbf{x} + \mathbf{v}_k. \tag{2.5}$$

After eliminating $\mathbf{x}$ from Eqn.2.5, we express Eqn.2.3 by rearranging it as follows,

$$\mathbf{Bg} = \mathbf{Dg}, \tag{2.6}$$

$$\mathbf{B} = \begin{bmatrix} [\mathbf{w}_2 & -\mathbf{w}_1 & \mathbf{0} & \cdots & \cdots & \mathbf{0}] \\ [\mathbf{w}_3 & \mathbf{0} & -\mathbf{w}_1 & \mathbf{0} & \cdots & \mathbf{0}] \\ & & \vdots & & & \\ [\mathbf{w}_L & \mathbf{0} & \cdots & \cdots & \mathbf{0} & -\mathbf{w}_1] \\ \hdashline [\mathbf{0} & \mathbf{w}_3 & -\mathbf{w}_2 & \mathbf{0} & \cdots & \mathbf{0}] \\ & & \vdots & & & \\ [\mathbf{0} & \mathbf{w}_L & \mathbf{0} & \cdots & \mathbf{0} & -\mathbf{w}_2] \\ \hdashline & & \vdots & & & \\ \hdashline [\mathbf{0} & \cdots & \cdots & \mathbf{0} & \mathbf{w}_L & -\mathbf{w}_{L-1}] \end{bmatrix}, \mathbf{D} = \begin{bmatrix} [\mathbf{w}_2 & -\mathbf{v}_1 & \mathbf{0} & \cdots & \cdots & \mathbf{0}] \\ [\mathbf{w}_3 & \mathbf{0} & -\mathbf{v}_1 & \mathbf{0} & \cdots & \mathbf{0}] \\ & & \vdots & & & \\ [\mathbf{w}_L & \mathbf{0} & \cdots & \cdots & \mathbf{0} & -\mathbf{v}_1] \\ \hdashline [\mathbf{0} & \mathbf{w}_3 & -\mathbf{v}_2 & \mathbf{0} & \cdots & \mathbf{0}] \\ & & \vdots & & & \\ [\mathbf{0} & \mathbf{w}_L & \mathbf{0} & \cdots & \mathbf{0} & -\mathbf{v}_2] \\ \hdashline & & \vdots & & & \\ \hdashline [\mathbf{0} & \cdots & \cdots & \mathbf{0} & \mathbf{w}_L & -\mathbf{v}_{L-1}] \end{bmatrix} \in C\left(\frac{N \times L(L-1)}{2} \times L\right), \tag{2.7}$$

$$\mathbf{g} = \{g_1 \quad \cdots \quad g_{j-1} \quad g_j \quad g_{j+1} \quad \cdots \quad g_{k-1} \quad g_k \quad g_{k+1} \quad \cdots \quad g_L\}^T, \tag{2.8}$$

where $\mathbf{g}$ indicates the transfer function vector of all measuring points with respect to the input signal $\mathbf{x}$. After performing a multiplication on both sides of $\mathbf{B}^*$ from left, and setting $\mathbf{\Sigma} = \mathbf{B}^*\mathbf{B}$ and $\mathbf{R} = \mathbf{B}^*\mathbf{D}$, we express Eqn.2.6 by rearranging it as follows,

$$(\mathbf{\Sigma} - \mathbf{R})\mathbf{g} = \mathbf{0}, \tag{2.9}$$

where * denotes the transposed complex conjugate. Eqn.2.9 represents the normal equation of the SIMO system corresponding to Eqn.2.6. A coefficient matrix $\mathbf{\Sigma} \in C(L \times L)$ can be written as,

$$\mathbf{\Sigma} = trace(\mathbf{S}) \cdot \mathbf{I} - conjg(\mathbf{S}), \tag{2.10}$$

where $\mathbf{I} \in R(L \times L)$ indicates a unit matrix. A covariance matrix $\mathbf{S} \in C(L \times L)$ indicates as follows,

$$\mathbf{S} = \begin{bmatrix} \mathbf{w}_1^*\mathbf{w}_1 & \cdots & \mathbf{w}_1^*\mathbf{w}_L \\ \vdots & \ddots & \vdots \\ \mathbf{w}_L^*\mathbf{w}_1 & \cdots & \mathbf{w}_L^*\mathbf{w}_L \end{bmatrix}. \tag{2.11}$$

The diagonal terms of $\mathbf{\Sigma}$ represent the summed up power spectrum, and the non-diagonal terms of $\mathbf{\Sigma}$ represent the summed up cross spectrum. $\mathbf{\Sigma}$ can constitute only measuring data. Under the assumption on the noises, Σ_{jj} and Σ_{jk} which are a diagonal and a non-diagonal terms of $\mathbf{\Sigma}$, respectively, represent as follows,

$$\Sigma_{jj} \approx \left(\sum_{l=1}^{L} \mathbf{y}_l^*\mathbf{y}_l\right) - \mathbf{y}_j^*\mathbf{y}_j + \left(\sum_{l=1}^{L} \mathbf{v}_l^*\mathbf{v}_l\right) - \mathbf{v}_j^*\mathbf{v}_j, \quad \Sigma_{jk} \approx -\mathbf{y}_k^*\mathbf{y}_j. \tag{2.12}$$

R_{jj} and $R_{jk}(j \neq k)$ which are a diagonal and a non-diagonal terms of $\mathbf{R}$, respectively, represent as,

$$R_{jj} \approx \left(\sum_{l=1}^{L} \mathbf{v}_l^*\mathbf{v}_l\right) - \mathbf{v}_j^*\mathbf{v}_j, \quad R_{jk} \approx 0. \tag{2.13}$$

The diagonal terms of $\boldsymbol{\Sigma}$ constitute both signal and noise. The diagonal terms of $\mathbf{R}$ constitute only noise. Noise reduction effect is expected at the non-diagonal terms of $\boldsymbol{\Sigma}$ and $\mathbf{R}$. Therefore, noises are summarized the diagonal terms of $\boldsymbol{\Sigma}$ and $\mathbf{R}$. Setting of $\mathbf{R} = \lambda \mathbf{R}_0$, Eqn.2.9 reduces to a eigenvalue problem, as follows,

$$(\boldsymbol{\Sigma} - \lambda \mathbf{R}_0)\mathbf{h} = \mathbf{0}. \tag{2.14}$$

$\mathbf{R}_0$ is parameter which can relatively estimate an amount of noises inclusive of the diagonal terms of $\boldsymbol{\Sigma}$, and its non-diagonal terms are zero. The minimum eigenvalue λ and its normalized eigenvector $\mathbf{h}$ can be obtained. The FRFs are identical with the eigenvector which is normalized by an element corresponding to a reference point. For example, the FRFs corresponding to the reference point l can be obtained as follows,

$$\mathbf{h}_l = \{h_1 \quad \cdots \quad h_{l-1} \quad 1 \quad h_{l+1} \quad \cdots \quad h_L\}^T = \{g_1/g_l \quad \cdots \quad g_l/g_l \quad \cdots \quad g_L/g_l\}^T \tag{2.15}$$

The above mentioned process estimates FRFs and a total amount of noises, names H_p estimation.

2.3.Estimation of Noise Quantity

In this paper, it is assumed that a total amount of noises proportion to a total amount of measurements,

$$\mathbf{R}_0 = \begin{bmatrix} \Sigma_{11} & & 0 \\ & \ddots & \\ 0 & & \Sigma_{LL} \end{bmatrix}. \tag{2.16}$$

The minimum eigenvalue λ denotes the ratio of a total amount of noises contained all measuring data under that assumption. The value of λ varies between zero and one. An estimated total amount of noise V_{all} can be written as follows,

$$V_{all} = \sum_{l=1}^{L} V_{ll} = \lambda \cdot trace(\mathbf{S}) = \lambda \cdot \sum_{l=1}^{L} S_{ll}. \tag{2.17}$$

An amount of noise can be estimated on an assumption that λ at all measuring points is same. For example, the noise power spectrum V_{ll} at measuring point l can be written as,

$$V_{ll} = \lambda \cdot S_{ll}. \tag{2.18}$$

The signal power spectrum can be estimated by eliminating the noise power spectrum from the diagonal terms of a covariance matrix $\mathbf{S}$.

2.4.The Merits of H_p estimation

1) An increase in the number of measuring points yields improvement in the estimating accuracy of the FRFs and the noises. Therefore, in case of application to the 2-output system, the accuracy is the lowest.
2) An increase in the number of measuring times improves the estimating accuracy of the FRFs and the noises, too.
3) Under an assumption that λ is the same value at all measuring points, the signal/noise power spectrum at each measuring point can be estimated. If the S/N ratio is known a priori, H_p estimation can be incorporated it into.

3. APPLICATION OF MICROTREMOR RECORDS TO AN EXISTING BRIDGE

3.1.Procedure

Figure 3 shows the estimation procedure of free vibration responses, which employs H_p estimation. H_p estimation is used to obtain the noises and the signal power spectrum. The Inverse Fourier transformation of this signal power spectrum and the cross spectrum produces the free vibration responses. H_p estimation does not limit input and noises to white waves and instead employs the signal power spectrum that further reduce noise disturbances. Furthermore, modal characteristics are identified by applying the Eigensystem Realization Algorithm (ERA, J.N. Juang, et al.1985) which is one of the EMA method to free vibration responses.

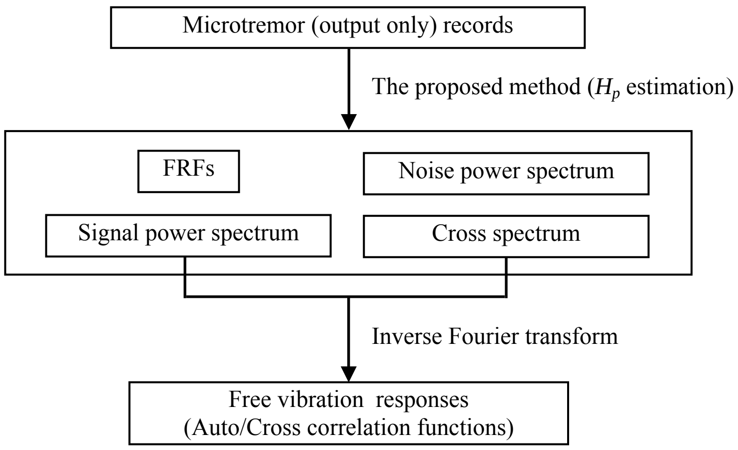

Figure 3 A flow of estimation of free vibration responses using H_p estimation.

3.2.The Summary of the Subject Bridge and Measurements

3.2.1 The subject bridge

Figure 4 outlines the subject bridge. It is supported by a total of 68 cables, with 17 cables in each single span on a single side. In design, it is a symmetric pre-stressed concrete cable-stayed bridge consisting of two continuous spans. Moving coil velocity vibrographs are used at 10 positions, as shown in Figure 4(2).

3.2.2 The summary of Vibration tests

Impact test: We placed the rear wheels of a dump truck which had the total weight of 107.4 kN (10.96 tf) at the position indicated by a ╳ in Figure 4(2). Then the wheels were dropped from a height of 10 cm, and the free vibration responses were measured. The sampling frequency was 100 Hz and the measuring time was approximately 1 minute.
Exciter test: We employed the “Rundown” method. We installed an eccentric weight exciter, which has a maximum exciting force of 98 kN (10 tf), at the position indicated with a ★ in Figure 4(2). We then applied an exciting force of 15 Hz in the vertical direction. Following this steady vibration, we measured responses until the power was cut off and the moving weight stopped completely. This measurement was conducted for approximately 1 minute using a sampling frequency of 120 Hz.
Microtremor observation: Using a sampling frequency of 100 Hz, we observed microtremors for 15 consecutive minutes. The measurement record of wind direction and velocity meter, which we observed simultaneously around the tower on the beam, showed that there was no wind present during the observation.

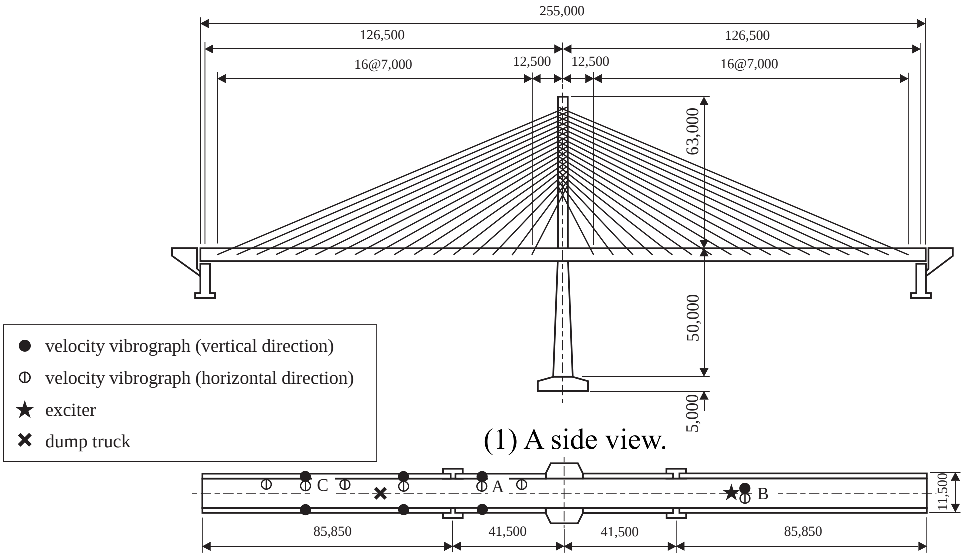

(unit: mm)

(1) A side view.

(unit: mm)

(2) A Floor view and measuring points.
Figure 4 An outline of the subject bridge.

3.3.The Numerical Analysis

Based on the results from the FVTs (Impact test and Exciter test), we carefully watched the vertical bending mode and constructed 3-dimensional finite element method (FEM) model for the subject bridge. We combined some beam elements using rigid bodies to join the tower and the cables, the tower and the beams, and the junction of the beams and the piers, while connecting the cables onto the beams with pins. Figure 5 shows the structure of the FEM model. Figure 6 shows examples of the mode shapes of the vertical bending and torsion modes obtained from the eigenvalue analysis of the FEM model. The vertical bending mode shows an anti-symmetric mode shape around the tower at an odd order, and one symmetric at an even order.

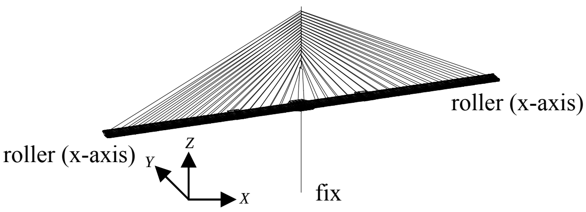

member	element
slab	solid
pier	beam
cable	chord

the total number of nodes = 8,792
the total number of elements = 5,583

Figure 5 The three dimensional finite element model.

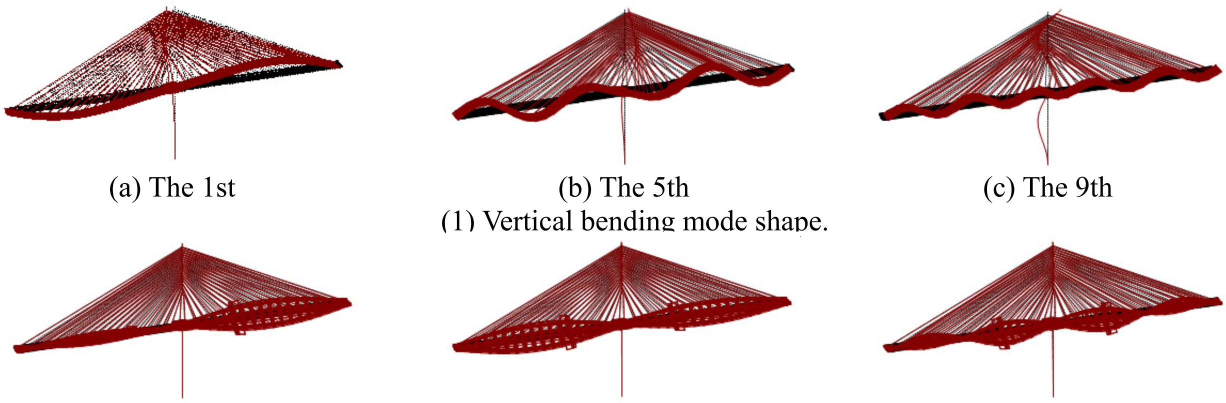

(a) The 1st (b) The 5th (c) The 9th
(1) Vertical bending mode shape.

(a) The 1st (b) The 5th (c) The 9th
(2) Torsion mode shape.
Figure 6 The mode shapes of the FEM model.

3.4.Application Results of H_p estimation to Microtremor Records

3.4.1 Signal/Noise power spectrum and estimation results of the FRFs

We divided the approximately 15-minute of continuous observation into 22 observation periods, each 40.96 s long. We then divided the components into vertical and horizontal elements and applied H_p estimation.
Figure 7 shows some of the power spectrum of the signals and noises obtained at measuring points A, B and C as examples. The vertical components were considered to be affected by noises in the valley bottom of the power spectrum. The peak points showed almost no influence from noises that were nearly consistent with the measurements. Figure 8 illustrates the FRF estimation results, with the point B as the reference point and the points A and C as the objective points.

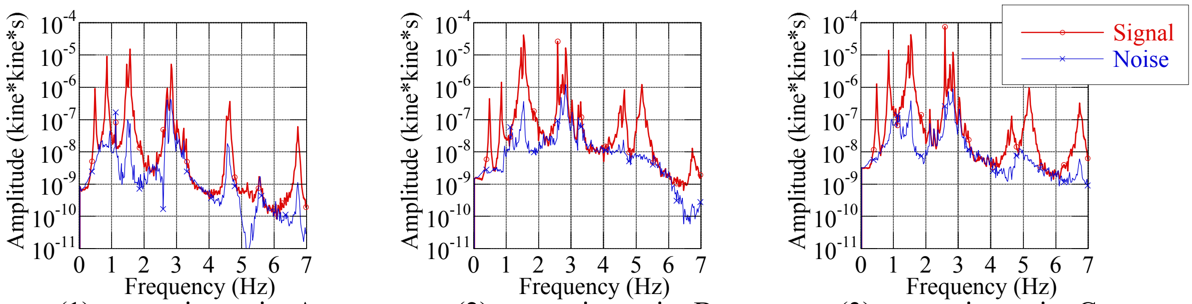

(1) measuring point A. (2) measuring point B. (3) measuring point C.

Figure 7 Signal/Noise power spectrum.

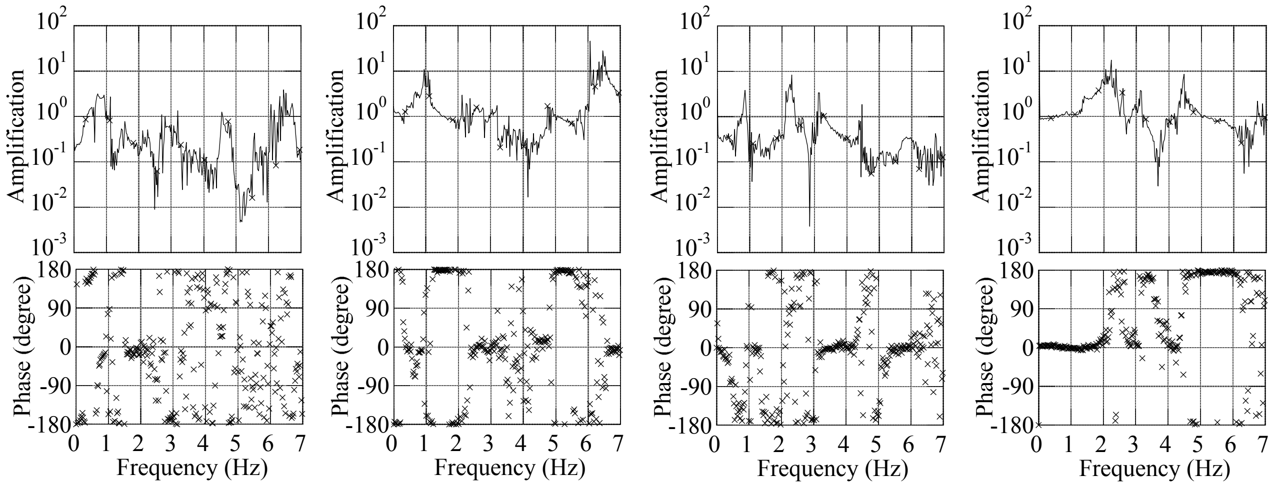

(a) point A/point B. (b) point C/point B. (a) point A/point B. (b) point C/point B.

(1) Vertical direction. (2) Horizontal direction.

Figure 8 FRFs.

3.4.3 Identification results of the modal characteristics

Figure 9 shows the natural frequency obtained in correspondence to the mode order. In spite of the short observation time, approximately 15 minutes, we detected a total of 14 modes using H_p estimation. The Figure also shows the natural frequency obtained from the FVTs and the FEM model.
The 1st through 3rd vertical bending modes coincided with the Impact test results, and the 1st through 4th and 6th through 8th vertical bending modes with the FVT results. Thanks to these, as for vertical bending modes excited in the FVTs, we could identify the natural frequency obtained by H_p estimation applied to the microtremor records with a similar level of precision with results from such high-precision measurements as FVTs.
The FEM model expresses the microtremor observation results well for the 10th vertical bending and the

torsion modes, for which the FVTs failed to provide data. With the horizontal mode, only the 1st mode was expressed. H_p estimation was unable to detect the 5th and 9th modes of vertical bending. Since the 5th mode of vertical bending was in close vicinity of the 1st and 2nd modes of torsion, and the 9th mode of vertical bending to the 3rd mode of torsion, it is estimated that H_p estimation lacked sufficient resolution to tell those apart during the approximate 15-minute microtremor observation. We also consider that these modes were insufficiently excited, since they were anti-symmetric modes, as shown in Figure 6.

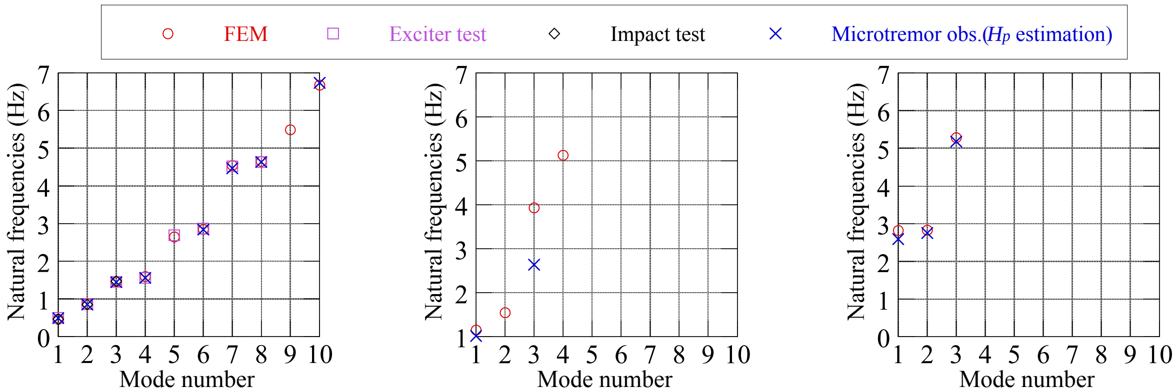

(1) Vertical bending mode. (2) Horizontal bending mode. (3) Torsional mode.

Figure 9 A Comparison FEM and vibration tests.

4. CONCLUSIONS

The FVTs are capable of more precise measurement than the microtremor observation, but request a great deal of labor and cost. The microtremor observation is needed a high precise data processing scheme although can be carried out relatively easily. In this paper, an availability of H_p estimation which has been proposed by the authors for estimating the FRFs and the noises from output only data is argued. H_p estimation was able to estimate more modes than those of the FVTs. The many modes identified by H_p estimation were very useful for constructing a high-precision numerical model. It proved that the precise modal characteristics were obtained by H_p estimation.

REFERENCES

Brincker R., Zhang L. and Andersen P. (2000). Modal identification from ambient responses using Frequency Domain Decomposition. *Proceedings of 18th International Modal Analysis Conference (IMAC-XVII)*. 625-630.

Peeters B. and De Roeck G. (1999). Reference-based stochastic subspace identification for output-only modal analysis. *Mechanical Systems and Signal Processing* **6:33**. 855-878.

B. Schwarz and M. Richardson. (2007). Using a De-Convolution Window for Operation Modal Analysis. *Proceedings of the 2nd International Operational Modal Analysis Conference* **1**. 13-22.

Farrar, C.R. and James, G.H. (1997). System Identification from Ambient Vibration Measurements on a Bridge. *Journal of Sound and Vibration* **205:1**. 1-18.

M. Izumi, H. Katukura and J. Tobita. (1990). Properties of ambient vibration system of structures. *Journal of Structural and Construction Engineering AIJ* **409**, 83-93 (in Japanese).

G.T. Rocklin., J. Crowely. and H. Vold. (1985). A comparison Of H1, H2, Hv Frequency Response Functions, *Proceedings of 3rd International Modal Analysis Conference (IMAC-III)*. 272-278.

M. Nakamura, J. Suzumura and K. Hanada. (2006). An evaluation method of frequency response functions through observed motions with noise. *Journal of Structural Engineering JSCE* **52A**, 219-226 (in Japanese).

J.N. Juang and R.S. Pappa. (1985). An Eigensystem Realization Algorithm for Modal Parameter Identification and Model Reduction. *Journal of Guidance, Control and Dynamics* **8:5**. 620-627.